



View-angle consistency in reflectance, optical thickness and spherical albedo of marine water-clouds over the northeastern Pacific through MISR-MODIS fusion

Lusheng Liang,¹ Larry Di Girolamo,¹ and Steven Platnick²

Received 30 December 2008; revised 19 March 2009; accepted 7 April 2009; published 9 May 2009.

[1] View-angle consistency in bidirectional reflectance factor (BRF), optical thickness and spherical albedo is examined for marine water clouds over a region of the northeastern Pacific using six years of fused Moderate Resolution Imaging Spectroradiometer (MODIS) and Multiangle Imaging SpectroRadiometer (MISR) data. Consistency is quantified by the root-mean-square of relative differences between MISR-measured BRF and their plane-parallel values and variation of plane-parallel retrieved optical thickness and spherical albedo across multiple view-angles. Probability distribution functions of consistency show that, for example, these clouds are angularly consistent within 5% in BRF, optical thickness and spherical albedo 72.2%, 39.0% and 81.1% of the time, respectively. We relate angular consistency to the spatial variability of nadir-BRF, thus allowing us to potentially identify, with a prescribed confidence level, which MODIS microphysical retrievals within the MISR swath meet the plane-parallel assumption to within any desired range in view-angle consistency. **Citation:** Liang, L., L. Di Girolamo, and S. Platnick (2009), View-angle consistency in reflectance, optical thickness and spherical albedo of marine water-clouds over the northeastern Pacific through MISR-MODIS fusion, *Geophys. Res. Lett.*, 36, L09811, doi:10.1029/2008GL037124.

1. Introduction

[2] All operational satellite retrievals of cloud optical properties from scattered solar radiances assume one-dimensional radiative transfer (1D-RT), whereby clouds and the imposed boundary conditions are treated as horizontally homogeneous (i.e., plane-parallel), with cloud layers usually assumed to be vertically homogenous. The applicability of this assumption has been examined through many observational [e.g., *Loeb and Davies*, 1996, 1997; *Loeb and Coakley*, 1998; *Genkova and Davies*, 2003; *Horváth and Davies*, 2004; *Várnai and Marshak*, 2007] and three-dimensional radiative transfer modeling [e.g., *Loeb et al.*, 1998; *Várnai and Davies*, 1999; *Kato et al.*, 2006] studies. However, the following fundamental question remains: how often is this assumption good enough? Clearly, “good enough” will depend on the application, and its answer will depend on, preferably, a globally representative dataset of true optical properties of clouds. Given the lack of such a dataset, we must seek alternative

ways to answer this question. Two recent studies, *Genkova and Davies* [2003] and *Horváth and Davies* [2004] have made such attempts. *Genkova and Davies* [2003] examined the spatial contrast of MISR red band BRF as a function of spatial scale and found that only a small fraction of the clouds were homogeneous for a range of spatial contrast thresholds. However, the spatial contrasts in BRF were not explicitly tied to the quality of cloud microphysical retrievals under the plane-parallel assumption. *Horváth and Davies* [2004] examined the anisotropy of water cloud BRF and found ~17% of cloudy pixels at 275 m resolution (~30% at 3.3 km resolution) had agreement between 1D-RT modeled BRFs and MISR-observed BRFs to within $\pm 5\%$ for all MISR view angles (See section 2.1 for MISR instrument description), when the views were coregistered to a constant altitude over 70.4 km² domains. However, there was no tie to the spatial heterogeneity of the scene, and it is not clear whether the $\pm 5\%$ threshold is appropriate for all applications.

[3] In this study, we extend the *Horváth and Davies* [2004] approach in several ways. Our approach fuses the MISR multi-angle radiances with the MODIS cloud optical thickness (τ) and effective radii (r_e) retrievals. Fusion is done at cloud top and at pixel resolution (~1 km², rather than a 70.4 km² domain) using a new cloud element registration scheme (section 2.2). Angular consistency metrics are defined (section 2.3) for BRF, τ and cloud spherical albedo (β) to ascertain the appropriateness of the 1D-RT assumption on different properties of the cloud. The metrics are applied to water clouds over a large region of the northeastern Pacific Ocean for data collected over six years, providing ample sampling to study the frequency of occurrence in the metric values and their relationship to cloud heterogeneity (section 3).

2. Data and Methodology

2.1. Instruments and Dataset

[4] MODIS, onboard the Terra and Aqua satellite platforms, retrieves τ and r_e across its 2330 km swath at a ground-resolution of 1 km at nadir [*Platnick et al.*, 2003]. MISR, also on Terra, provides nine views of the same scene on Earth within seven minutes from its multi-camera design, with view zenith angles of 0°, $\pm 26.1^\circ$, $\pm 45.6^\circ$, $\pm 60.0^\circ$, and $\pm 70.5^\circ$ along the forward and aft directions of the orbital-track [*Diner et al.*, 1998]. BRFs are measured at 4 spectral channels (three visible and one near-infrared), with the ground resolution varying from 275 m to 1.1 km, depending on the channel, across a swath of ~400 km that falls near the center of the MODIS swath.

[5] MISR and MODIS data were extracted from Path 47 and 48 of Terra within a region bound by 9.8°N to 40.3°N

¹Department of Atmospheric Sciences, University of Illinois at Urbana-Champaign, Urbana, Illinois, USA.

²Laboratory for Atmospheres, NASA Goddard Space Flight Center, Greenbelt, Maryland, USA.

and 122.7°W to 137.4°W at approximately 10:30 am local time as defined by the sun-synchronous orbit of Terra. This region is dominated by stratus and stratocumulus to the north and transitions to trade wind cumuli and deeper cumuli to the south, although other cloud types are also noted [e.g., *Hahn and Warren*, 1999]. 302 orbits from May 2000 to April 2006 were used in this study. Version 24 of the MISR Level 1B2 georectified and calibrated near-infrared (0.86 μm) BRFs and the MODIS Collection 5 near-infrared (0.86 μm) BRF, MOD06 τ , r_e , and cloud phase flag were used in our analysis. Only water clouds were considered in our analysis based on the cloud phase flag. The MODIS Collection 5 cloud retrieval algorithm does not process cloud edges (as determined from the MODIS cloud mask, MOD35). These edge pixels are therefore excluded from our analysis.

2.2. Cloud Element Registrations

[6] The MODIS BRF, τ and r_e reported at 1 km resolution on the MODIS swath are registered to the MISR 1.1 km resolution grid with the General Cartographic Transformation Package software [*U.S. Geological Survey*, 1993]. To reduce registration errors of cloud elements originating on different grids, we define a domain as a region consisting of 3×3 1.1 km pixels (justified in next paragraph) with all nine pixels having successful τ and r_e retrievals. Our analysis shows that these domains contain 79.5% of all pixels having successful $\tau - r_e$ -retrievals, since not all successful $\tau - r_e$ -retrievals fall within 3×3 pixel domains that are fully cloudy. The relative difference between the BRF from the MISR nadir camera and from MODIS is given by

$$\delta_{OBS} = \frac{(\bar{R}_{MISR_NADIR} - \bar{R}_{MODIS})}{(\bar{R}_{MISR_NADIR} + \bar{R}_{MODIS})/2} \times 100\%,$$

where \bar{R}_{MISR_NADIR} and \bar{R}_{MODIS} are average near-infrared BRFs for MISR-nadir camera and MODIS over a domain, respectively. When averaged over all domains in our dataset, $\delta_{OBS} = 1.37\%$ with a standard deviation (σ) of 4.74%. The non-zero value of δ_{OBS} arises from differences in the spectral response function and radiometric calibration between MISR and MODIS, whereas registration errors also contribute to σ [e.g., *Lyapustin et al.*, 2007]. The impact of registration errors could be reduced by accepting only those domains having a δ_{OBS} within $\delta_{OBS} \pm \sigma$; 78.8% of domains meet this criterion. We refer to this as the MODIS-MISR registration criterion (MMRC).

[7] We also need to register cloud elements across MISR images acquired from multiple view directions. Because of the way MISR projects and regrid its BRFs from all cameras to a common Space-Oblique Mercator (SOM) grid on the World Geodetic System 1984 ellipsoid surface, it is possible that a BRF from a cloud fully covering a single pixel in a nadir camera image be split over two pixels in an oblique camera image, and the BRFs from a cloud fully covering M pixels in the nadir camera is split over $M + 1$ pixels [*Jovanovic et al.*, 1999]. The same is also true when reprojecting MODIS data onto the MISR grid. Thus, averaging the BRFs over larger areas helps alleviate this problem. For this reason, we choose 3×3 1.1 km pixels as our domain size throughout our analysis.

[8] Identifying the same cloud across MISR images from multiple views is equal to finding the cloud displacements

(parallaxes) in the oblique images relative to the nadir image on the SOM grid. We use the MISR area-matching algorithm M2 [*Muller et al.*, 2002] and implement it as follows to increase reliability in the match (but at the expense of coverage). At 1.1 km resolution, for every pixel in the nadir image that belongs to a domain, we center a 7×11 -pixel patch on it and compare the patch to all 7×11 -pixel patches within a large search window in an oblique image. Where a patch in the oblique image best matches the nadir target patch based on the M2 criteria (using a minimum M2 covariance value), the center pixel on the patch in the oblique image is registered to the target pixel in the nadir image. Because the magnitude and direction of the parallax will depend on the altitude and wind vector of the cloud, we require that all 9 pixels belonging to a domain return the same parallax. When this requirement is not met, a larger patch is used to yield more accurate registration (at the cost of more computation) as recommended by *Muller et al.* [2002]. Thus, we further increase the patch sizes from 7×11 pixels in increments of 2 pixels in both the along and cross track directions (i.e., 9×13 , and up to 17×21) until the 9-pixel parallax agreement is met, otherwise, the domain is discarded from our analysis.

[9] Matching clouds in the oblique images to the target clouds in the nadir image becomes more difficult with view obliquity, largely because the texture of clouds change with view angle. For fully cloudy domains, 65.4% had all 9 cameras meet the multi-camera registration requirement. In this study we exclude the two 70.5° MISR cameras, resulting in a registration rate for the remaining 7 cameras of 76.1%. Hereafter, we refer to this as the 7-MISR-camera registration criterion (7MRC). An increase in the quality of the registration can be had by first applying MMRC followed by 7MRC, hereafter referred to as MMRC+7MRC; 59.8% of all fully cloudy domains passed this registration criterion. Domains that have passed a registration criterion are referred to as qualified domains. Both qualified and unqualified domains for the different registration criteria will be examined in section 3.

2.3. Angular Consistency Metrics

[10] We first retrieve τ using the near-infrared BRF from the MISR nadir camera and r_e from MODIS, based on the same radiative transfer model used to construct the look-up tables in the MODIS τ and r_e retrievals [*King et al.*, 1997]. The BRFs for the seven MISR view angles are then simulated using the MISR τ and MODIS r_e . Within a domain, the observed MISR BRFs and simulated BRFs are averaged and designated \bar{R}_i^{OBS} and \bar{R}_i^{SIMU} , respectively, where i is the MISR camera index ($i = \{1, 2, \dots, 7\}$). If clouds are truly plane-parallel and meet all assumptions used by the MODIS microphysical retrieval algorithm, then we would expect the relative difference between \bar{R}_i^{OBS} and \bar{R}_i^{SIMU} , $\delta R_i = \frac{\bar{R}_i^{OBS} - \bar{R}_i^{SIMU}}{\bar{R}_i^{OBS}}$, to be close to zero for all values of i . The root-mean-square of the absolute value of δR_i from all chosen cameras defines the BRF angular consistency metric:

$$m_{BRF} = \sqrt{\frac{1}{n} \sum_{i=1}^n |\delta R_i|^2} \times 100\%, \quad (1)$$

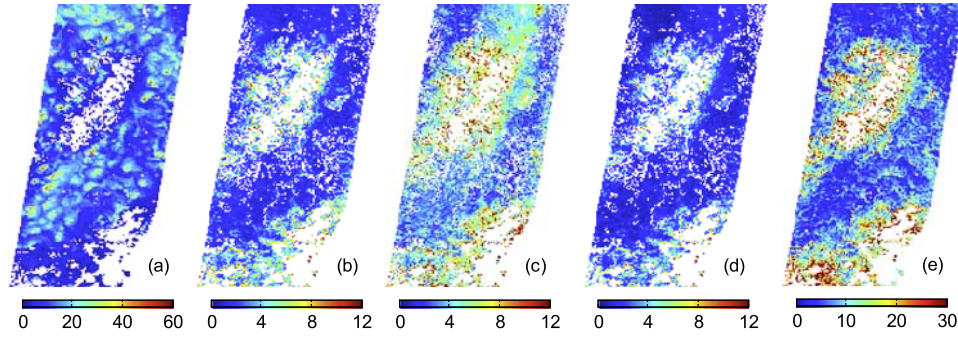


Figure 1. Examples of (a) the mean cloud optical depth, (b) m_{BRF} metric, (c) m_{τ} , (d) m_{β} and (e) H_{σ} for domains composed of $3 \times 3 - 1.1$ km pixels. The data are for MISR block 68 to 74, orbit 14700, collected on 22 September 2002 within 19.8°N to 21.1°N and 128.5°W to 133.8°W . White represents regions where domains do not meet the MODIS-MISR or 7-camera registration criterion.

where $n = 7$ is the number of MISR cameras used in the calculation.

[11] Alternatively, τ and β can be retrieved for all MISR cameras. Since τ and β should not be a function of view geometry for plane-parallel clouds, angular consistency metrics can be defined by the coefficient of variation of the retrieved τ or β :

$$m_x = \frac{1}{\langle \bar{x}_i \rangle} \sqrt{\frac{1}{n-1} \sum_{i=1}^n (\bar{x}_i - \langle \bar{x}_i \rangle)^2} \times 100\%, \quad (2)$$

where x is either τ or β , \bar{x}_i is the average τ or β over a domain in the i th MISR camera and $\langle \rangle$ denotes averaging over the n cameras. We infer β from plane-parallel calculation using τ and r_e as input.

[12] These metrics should not be interpreted as an estimation of the uncertainty in the MODIS microphysical retrievals. Rather, they simply quantify the angular consistency from BRF, τ and β . As such, they point to the degree to which the plane-parallel assumption and other assumptions used by the MODIS retrieval algorithm are valid. However, larger metric values should go hand-in-hand with lower confidence in the quality of the MODIS microphysical retrievals and the associated estimate of uncertainty [Platnick *et al.*, 2005] found in the product.

3. Results

[13] As an example of the spatial characteristics of the metrics, Figure 1 shows $\bar{\tau}$ retrieved from nadir, m_{BRF} , m_{τ} and m_{β} , as well as a spatial heterogeneity metric, H_{σ} , defined below. Figure 1 gives a sense that large values of the metrics occur for regions near cloud edges, small clouds and thin clouds, whereas small values of the metrics occur for central regions of thicker extensive clouds. This is consistent with the expectation that thick, extensive clouds should be the most appropriate clouds for the validity of the plane-parallel assumption and the least sensitive to the treatment of ocean reflectance in the retrieval.

[14] Figures 2a, 2b, and 2c show the probability distribution functions (PDF) and cumulative PDFs in the occurrence of m_{BRF} , m_{τ} and m_{β} . We see that clouds for the qualified MMRC+7MRC domains in our dataset are angu-

larly consistent in BRF to within 5% of their plane-parallel value 78.5% of the time and are angularly consistent to within 5% in τ and β 44.3% and 85.9% of the time, respectively. For metric values $\leq 10\%$, the angular consistency rates increase to 96.1%, 84.5% and 97.8% for m_{BRF} , m_{τ} and m_{β} , respectively. The angular consistency rate of 78.5% for the $m_{BRF} \leq 5\%$ is nearly three times as high as that shown in Figure 2 of Horváth and Davies [2004], where about 30% pixels are angularly consistent at 3.3 km resolution. Although the disagreement may be attributed to clouds over different regions as compared to their study (i.e., they used data between 60°N and 60°S from 28 MISR orbits collected in two days), the following additional differences are also relevant: (1) metrics defined here reflect the overall consistency at all chosen view angles rather than any single view angle; (2) we exclude the two most oblique cameras where confidence in the registrations is lower than in the less oblique cameras; (3) MISR cameras are registered at cloud tops rather than at a single altitude over 70.4 km^2 regions; and (4) cloud edge pixels, pixels not included in a domain and pixels in the unqualified domains are excluded from our analysis.

[15] Since biases of the 1D-retrieved cloud optical properties depend on cloud spatial heterogeneity, so too must the angular consistency. We tested several spatial metrics and found that spatial metrics based on the high resolution (275m) BRFs from the MISR nadir camera provided the simplest and best single-variable relationships with the angular consistency metrics. One such heterogeneity metric is defined as:

$$H_{\sigma} = \frac{\sigma}{\bar{R}},$$

where \bar{R} is the domain's mean BRF with a standard deviation of σ .

[16] Recall that the unqualified MMRC+7MRC domains represent $\sim 40\%$ of all domains. The PDF of H_{σ} for the unqualified MMRC+7MRC domains (not shown) is skewed towards larger values compared to the qualified MMRC+7MRC domains. This is because the MMRC favors rejecting more heterogeneous clouds, while, to a lesser extent for the sampled clouds, the 7MRC favors rejecting more homogeneous clouds. If we assume that within a narrow H_{σ} -bin, the angular consistency metric

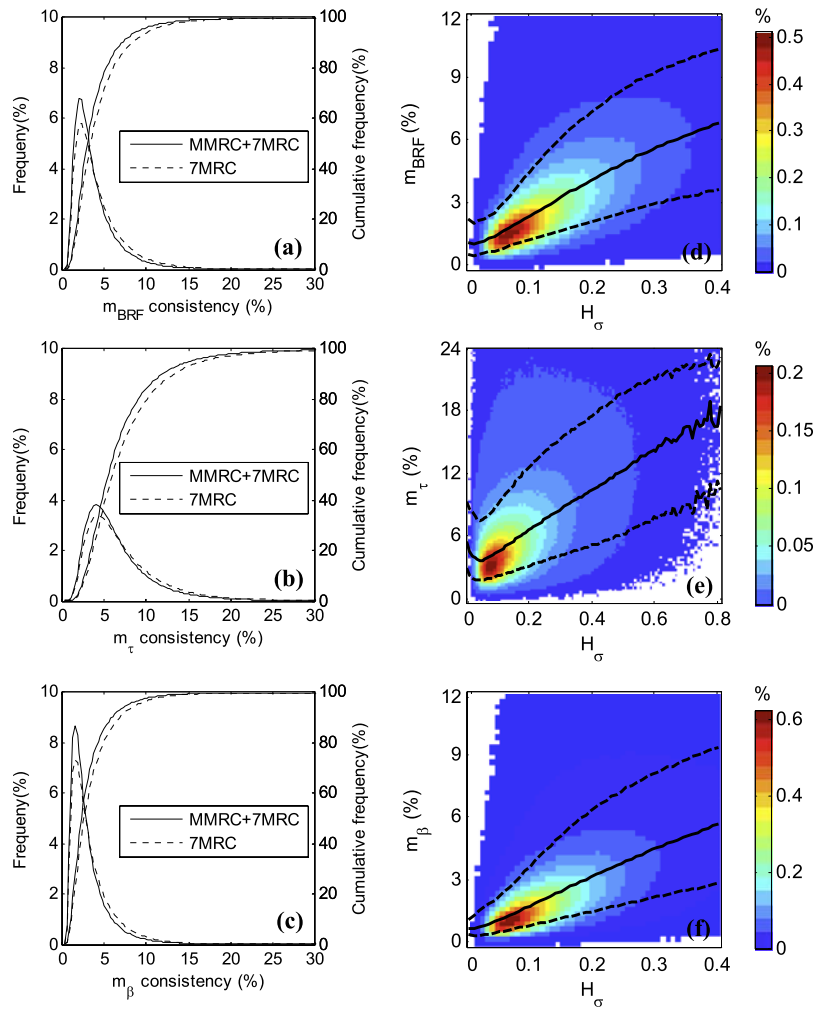


Figure 2. Probability distribution functions (PDF) and cumulative PDFs in (a) m_{BRF} , (b) m_{τ} , and (c) m_{β} metric for qualified MMRC+7MRC and 7MRC domains. 2-D frequency distribution of H_{σ} versus (d) m_{BRF} , (e) m_{τ} , and (f) m_{β} metric, for 7MRC domains. The median (solid thick line), 10th and 90th percentile (dotted lines) of the angular consistency metrics computed over H_{σ} bin intervals of 0.008 are also plotted.

PDFs are the same for both the qualified and unqualified MMRC+7MRC domains, then the angular consistency performance of the unqualified MMRC+7MRC domains can be predicted based on the PDF of H_{σ} . Following this method, we predict for metric values $<5\%$ (10%) consistency rates of 73.0% (94.4%), 40.0% (81.1%) and 81.7% (96.8%) for m_{BRF} , m_{τ} and m_{β} , respectively, for all domains. Compared to angular consistency rates derived from the qualified MMRC+7MRC domains, the differences are within 6%.

[17] When MMRC is omitted (only 7MRC is applied), lower consistency rates are expected for metric value $<5\%$ (10%) compared with those of qualified MMRC+7MRC domains, as showed in Figures 2a, 2b, and 2c: they are 71.7% (94.1%), 38.7% (79.9%) and 80.7% (96.7%) for m_{BRF} , m_{τ} and m_{β} , respectively, for the qualified 7MRC domains. Consistency rates are estimated for the unqualified 7MRC domains using the method described in the paragraph above, leading to consistency rates for all fully cloudy domains of 72.2% (94.3%), 39.0% (80.2%) and 81.1% (96.8%) in m_{BRF} , m_{τ} and m_{β} , respectively, for metric value $<5\%$ (10%). Note that the differences with the qualified-only 7MRC domains are less than 1%. The differences are also less than $\sim 1\%$

compared to the consistency rates estimated in the paragraph above for all domains using MMRC+7MRC. These small differences indicate that our analysis applied to the qualified 7MRC domains alone produces essentially unbiased results relative to the population of all fully cloudy domains.

[18] Figure 1 gives a clear sense that large values of H_{σ} are associated with large values of the angular consistency metrics. This is further quantified in Figures 2d, 2e, and 2f, which shows the 2-D distribution between angular consistency metrics and H_{σ} for the qualified 7MRC domains. As the cloud becomes more spatially heterogeneous within the domain (i.e., as H_{σ} increases), the mode and spread of the angular consistency metrics become larger. Analyses based on Figures 2d, 2e, and 2f show that for the 10% most spatially homogeneous domains, m_{BRF} and m_{β} are $<\sim 2\%$ and m_{τ} is $<\sim 15\%$ almost all the time. For the 10% most spatially heterogeneous domains, m_{BRF} , m_{τ} and m_{β} are $<\sim 5\%$ for $\sim 32\%$, 8% and 49% of the time, respectively. The relationship between the angular consistency and cloud spatial heterogeneity suggests the viability of using a cloud spatial heterogeneity criterion, based on MODIS observations falling in the MISR swath, for identifying

pixels that are not “good enough” for performing 1D-retrievals. For example, requiring 99% of the retrievals to be angularly consistent in BRF to within 5% of their plane-parallel value (i.e., $m_{BRF} \leq 5\%$; analogous to the 5% “good enough” criterion imposed by Horváth and Davies [2004] discussed in section 1), suggests performing retrievals only where $H_\sigma < 0.08$; $\sim 17.7\%$ of domains met this criterion.

4. Discussion

[19] We have examined the view-angle consistency in BRF, τ and β for marine water-clouds over the northeastern Pacific using six years of MISR and MODIS data. The clouds were sampled at the 10:30 am equator-crossing time of the Terra orbit. PDFs of metrics defining angular consistency quantify the plane-parallel nature of these clouds, allowing one to set thresholds on what they would deem “good enough” to be plane-parallel. For example, setting thresholds for all metrics at 5%(10%), the clouds in our dataset are angularly consistent in MISR-observed BRF to their plane-parallel values 72.2%(94.3%) of the time and to within 5%(10%) in τ and β 39.0%(80.2%) and 81.1%(96.8%) of the time, respectively. The results for 5% consistency in m_τ (39.0%) and in m_{BRF} (81.1%) may seem inconsistent; however, this is likely attributed to the non-linear relationship between BRF and τ . The angular consistency metrics was also shown to be associated with spatial heterogeneity. This allows one to set thresholds in spatial heterogeneity to identify, at a prescribed confidence level, which domains are angularly consistent to within a desired range (e.g., requiring $\sim 99\%$ of the retrievals to be angularly consistent in BRF to within 5% of their plane-parallel value suggests performing retrievals only where H_σ is < 0.08).

[20] Although the angular consistency depends, on average, on the spatial heterogeneity of the cloud field, it is by no means the only factor determining the magnitude of the angular consistency, as indicated by the spread of data in Figures 2d, 2e, and 2f. For example, there are some very smooth clouds that have large angular consistency metrics. This can potentially arise from deviations from other assumptions/inputs used in the MODIS plane-parallel retrievals of cloud microphysical properties, such as an assumed vertically homogeneous distribution of cloud microphysical properties, an assumed lambertian surface, and a correct classification of cloud phase. There are also a small number of clouds that are spatially heterogeneous with small angular consistency metrics, which we are only able to attribute to chance.

[21] Note that the results are derived at 3.3 km resolution only. Horváth and Davies [2004] demonstrated that angular consistency, akin to m_{BRF} , depends on resolution, with clouds appearing more plane-parallel with coarser resolution. We anticipate a similar behavior in our results, but this remains to be proven.

[22] Finally, the approach we have taken to assess the validity of the plane-parallel and other assumptions used in the MODIS retrievals is not limited to clouds over the northeastern Pacific. We are in the process of applying our approach to a global dataset to provide a broader perspective on this problem.

[23] **Acknowledgments.** This work was supported by a NASA Earth and Space Science Fellowship and a NASA New Investigator Program in Earth Science award, both under Program Manager Ming-Ying Wei. Additional support from the MISR project through the Jet Propulsion Laboratory of the California Institute of Technology is also gratefully acknowledged. We also thank two anonymous reviewers for their insightful comments. The MISR data were obtained from NASA Langley Research Center Atmospheric Sciences Data Center. The MODIS data were obtained through the Level 1 and Atmosphere Archive and Distribution System of NASA Goddard Space Flight Center.

References

- Diner, D. J., et al. (1998), Multiangle Imaging Spectroradiometer (MISR) description and experiment overview, *IEEE Trans. Geosci. Remote Sens.*, *36*, 1072–1087.
- Genkova, I., and R. Davies (2003), Spatial heterogeneity of reflected radiance from globally distributed clouds, *Geophys. Res. Lett.*, *30*(21), 2096, doi:10.1029/2003GL018194.
- Hahn, C. J., and S. G. Warren (1999), Extended Edited Synoptic Cloud Reports from Ships and Land Stations over the Globe, 1952–1996, http://gcmd.nasa.gov/records/GCMD_CDIA_CNDP026C.html, Carbon Dioxide Inf. Anal. Cent., Oak Ridge Natl. Lab., Oak Ridge, Tenn.
- Horváth, A., and R. Davies (2004), Anisotropy of water cloud reflectance: A comparison of measurements and 1D theory, *Geophys. Res. Lett.*, *31*, L01102, doi:10.1029/2003GL018386.
- Jovanovic, V. M., S. Lewicki, M. Smyth, J. Zong, and R. Korechoff (1999), Level 1 georectification and registration algorithm theoretical basis, *JPL Publ.*, D-11532.
- Kato, S., L. M. Hinkelman, and A. Cheng (2006), Estimate of satellite-derived cloud optical thickness and effective radius errors and their effect on computed domain-averaged irradiances, *J. Geophys. Res.*, *111*, D17201, doi:10.1029/2005JD006668.
- King, M. D., S.-C. Tsay, S. E. Platnick, M. Wang, and K. N. Liou (1997), Cloud retrieval algorithms for MODIS: Optical thickness, effective particle radius, and thermodynamic phase, *MODIS Algorithm Theor. Basis Doc. ATBD-MOD-05*, NASA Goddard Space Flight Cent., Greenbelt, Md.
- Loeb, N. G., and J. A. Coakley Jr. (1998), Inference of marine stratus cloud optical depths from satellite measurements: Does 1D theory apply?, *J. Clim.*, *11*, 215–233.
- Loeb, N. G., and R. Davies (1996), Observational evidence of plane parallel model biases: Apparent dependence of cloud optical depth on solar zenith angle, *J. Geophys. Res.*, *101*, 1621–1634.
- Loeb, N. G., and R. Davies (1997), Angular dependence of observed reflectances: A comparison with plane parallel theory, *J. Geophys. Res.*, *102*, 6865–6881.
- Loeb, N. G., T. Várnai, and D. M. Winker (1998), Influence of subpixel-scale cloud-top structure on reflectances from overcast stratiform cloud layers, *J. Atmos. Sci.*, *55*, 2966–2973.
- Lyapustin, A., Y. Wang, R. Kahn, J. Xiong, A. Ignatov, R. Wolfe, A. Wu, B. Holben, and C. Bruegge (2007), Analysis of MODIS-MISR calibration differences using surface albedo around AERONET sites and cloud reflectance, *Remote Sens. Environ.*, *107*, 12–21.
- Muller, J.-P., A. Mandanayake, C. Moroney, R. Davies, D. Diner, and S. Paradise (2002), MISR stereoscopic image matchers: Techniques and results, *IEEE Trans. Geosci. Remote Sens.*, *40*, 1547–1559.
- Platnick, S., M. D. King, S. A. Ackerman, W. P. Menzel, B. A. Baum, J. C. Riedi, and R. A. Frey (2003), The MODIS cloud products: Algorithms and examples from Terra, *IEEE Trans. Geosci. Remote Sens.*, *41*, 459–473.
- Platnick, S., R. Pincus, B. Wind, M. D. King, M. Gray, and P. Hubanks (2005), An initial analysis of the pixel-level uncertainties in global MODIS cloud optical thickness and effective particle size retrievals, *Proc. SPIE*, *5652*, 1–12.
- U.S. Geological Survey (1993), General Cartographic Transformation Package (GCTP), U.S. Geol. Surv., Reston, Va.
- Várnai, T., and R. Davies (1999), effects of cloud heterogeneities on short-wave radiation: Comparison of cloud-top variability and internal heterogeneity, *J. Atmos. Sci.*, *56*, 4206–4224.
- Várnai, T., and A. Marshak (2007), View angle dependence of cloud optical thicknesses retrieved by Moderate Resolution Imaging Spectroradiometer (MODIS), *J. Geophys. Res.*, *112*, D06203, doi:10.1029/2005JD006912.

L. Di Girolamo and L. Liang, Department of Atmospheric Sciences, University of Illinois at Urbana-Champaign, 105 S. Gregory Street, Urbana, IL 61801, USA. (lliang4@atmos.uiuc.edu)

S. Platnick, Laboratory for Atmospheres, NASA Goddard Space Flight Center, Code 613.2, Greenbelt, MD 20771, USA.